Available online at www.sciencedirect.com

ScienceDirect

materialstoday: PROCEEDINGS

www.materialstoday.com/proceedings

Materials Today: Proceedings 1 (2014) 17 – 24

The 1st International Joint Mini-Symposium on Advanced Coatings between Indiana University-Purdue University Indianapolis and Changwon National University

Lamellar to Rod Eutectic Transition in the Hypereutectic Nickel-Aluminum Alloy

Z.P. Que[a], J.H. Gu[a], J.H. Shin[b], H.K. Choi[a], Y.G. Jung[a], J.H. Lee[a,*]

[a]*Department of Materials Science & Engineering, Changwon National University, 20 Changwondaehak-ro, Uichang-gu, Changwon, Gyeongnam 641-773, Korea*

[b]*Doosan Heavy Industries & Construction Co. Ltd., Casting & Forging Process Technology Development Team, 22 DoosanVolvo-ro, Seongsan-gu, Changwon, Gyeongnam 642-792, Korea*

Abstract

Directional solidification experiments were carried out on the hypereutectic Ni-25 at.% Al alloy to examine the effect of growth velocity on the eutectic microstructure. The growth velocity was varied from 1 to 20 μm/s at a constant temperature gradient of 10.0 K/mm. The microstructural observations of unidirectionally solidified samples show that the lamellar eutectic growth was observed in the sample solidified at a constant velocity of 1 μm/s and the rod eutectic growth at velocities higher than 10 μm/s. A microstructural transition from lamellar to rod eutectics was achieved at the intermediate velocity. The lamellar to rod eutectic transition was shown to result from the compositional change due to the presence of strong convection in the melt. The undercooling-spacing curves showed that the average eutectic spacings for the lamellar and the rod structures were 1.6 times larger than that in the minimum undercooling for a given velocity.

Keywords: Ni-Al alloy ; Eutectic ; Directional solidification ; Undercooling ; Interphase spacing

* Corresponding author. Tel.: +82-55-213-3695 ; fax: +82-55-261-7017.
E-mail address: ljh@changwon.ac.kr

doi:10.1016/j.matpr.2014.09.004

1. Introduction

In recent years, many researchers [1-4] have studied the effect of convection on the solidification microstructure. Convection effects driven by density differences in the melt fall generally into two categories, depending on the origin of driving force: Convection by a lateral density gradient and convection by a vertical density gradient. During the solidification of alloys, the solute atoms are rejected at the solid/liquid interface when the equilibrium distribution coefficient is fewer than unity. If the rejected solute at the interface is heavier than the solvent, thermosolutal convection leads to high levels of solute segregation in the radial direction during upward directional solidification. This indicates that the microstructure should be different at each radial position on the interface [4]. However, the solute profile in the alloy systems with lighter solutes is quite homogeneous over the radial direction except in the immediate region of the tube wall, indicating that the interface microstructure should be uniform at each radial position [5]. It keeps changing with solid fraction under a constant growth velocity during the solidification process.

The theoretical model for the growth and stability of lamellar and rod eutectic microstructures were first established by Jackson and Hunt [6]. It involves that the eutectic growth occurs at the minimum undercooling possible, maintaining a balance between solutal and curvature undercoolings. The relationships between eutectic spacing and growth velocity were examined for Pb-Au, Pb-Pd, Pd-Cd and Pb-Sn alloys [7], showing that eutectic phases are not stable at a constant spacing corresponding to the minimum undercooling but rather within a certain range between minimum and maximum spacings. Trivedi et al. [8] studied on the eutectic spacing in the three dimensional eutectic growth under a diffusive growth condition. They found that the ratio of maximum to minimum spacing in three dimensions obeys 1.2 instead of 2.0, where 2.0 was predicted from two dimensional convective systems [7,9]. A similar study showed that convection exerts no significant influence on the eutectic spacing in Al-Cu alloys near the eutectic composition [10].

The vertical composition variations by convection can alter the interface microstructure, e.g., the transition from single phase to eutectic and from lamellar to rod eutectic or from rod to lamellar eutectic. The purpose of this study is to investigate the dependence of growth velocity on the microstructural evolution during the directional solidification of the hypereutectic Ni-25.2 at.% Al alloy. By the comparison of microstructures with different growth velocities, it is shown that melt convection leads to the transition of lamellar to rod eutectic microstructures under the constant thermal gradient.

2. Experimental

A Ni-based alloy with 25.2 at.% Al was prepared from 99.998 % purity nickel and 99.999 % purity aluminum by vacuum induction melting. The eutectic composition in the binary Ni-Al system is shown on the phase diagram [11] in Fig. 1 to be 24.5 at.% Al and the Ni-Al alloy used in the present study is slightly off of the exact eutectic composition. The thermo-physical parameters for the Ni-Al systems used for calculation are shown in Table 1 [11,13]. 100-mm-long cylindrical rods were machined from the as-cast ingot to fit into an alumina tube with an inner diameter of 5 mm for the directional solidification experiments. Upward directional solidification was performed in a modified Bridgman type furnace [12]. An alumina tube containing a sample rod was mounted into a water cooling jacket at the lower part and fixed at the top of the furnace assembly. The alumina tube was first evacuated to eliminate oxygen and filled with high-purity argon gas to a pressure of 10 psi. After flushing three times, the furnace was heated up to 1500 °C and held for 30 minutes to stabilize the solid/liquid interface. The rate of solidification was limited to 20 μm/s because the dendrites of the primary β phase were found to occur at velocities faster than 30 μm/s. The thermal gradient in the liquid at the solid/liquid interface was repeatedly measured by a B-type thermocouple to be 10.0 K/mm. When the volume fraction of the solid phase solidified in a given growth condition reached roughly 0.6, the alumina tube was quickly dropped into a water bath to preserve the solidifying interface.

The solidified samples were metallographically prepared and etched in Marble's reagent made up of 10 g of $CuSO_4$, 50 ml of HCl and 50 ml of H_2O. Longitudinal and transverse microstructures were observed using an optical microscope. The energy dispersive spectrometer (EDS) on scanning electron microscope (SEM) was used to measure the concentration of Al element. Both microstructural observations and the composition analyses were

made in the central part of the solidified samples to avoid the segregation effect in the radial direction driven by convection.

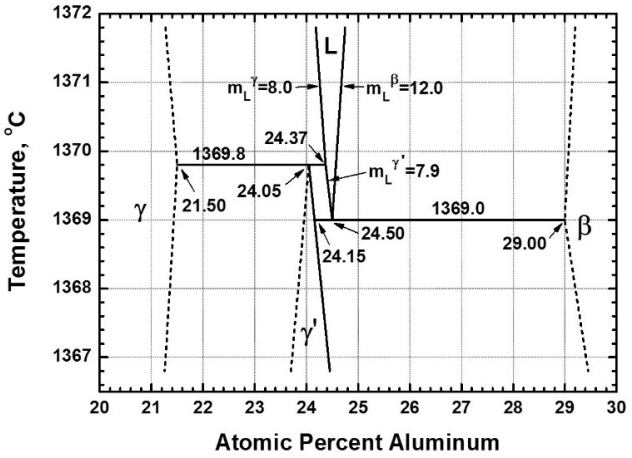

Fig. 1. Binary Ni-Al phase diagram.

Table 1. Physical properties of the Ni-Al alloy.

Parameter	Value	Unit	Reference
γ phase			
Gibbs-Thomson coefficient, Γ_γ	1.73×10^{-7}	(m·K)	[13]
Liquidus slope, m_γ	8	(K/at.% Al)	[11]
Distribution coefficient, k_γ	0.88		[11]
γ′ phase			
Gibbs-Thomson coefficient, $\Gamma_{\gamma'}$	2.71×10^{-7}	(m·K)	[13]
Liquidus slope, $m_{\gamma'}$	7.9	(K/at.% Al)	[11]
Distribution coefficient, $k_{\gamma'}$	0.986		[11]
β phase			
Gibbs-Thomson coefficient, Γ_β	1.75×10^{-7}	(m·K)	[13]
Liquidus slope, m_β	12	(K/at.% Al)	[11]
Distribution coefficient, k_β	1.184		[11]
β-γ eutectic			
Eutectic temperature, T	1369.00	(°C)	[11]
Eutectic composition	24.5	(at.% Al)	[11]
Contact angle for γ, θ_γ	50.4	(°)	[13]
Contact angle for β, θ_β	6.3	(°)	[13]
β-γ′ eutectic			
Eutectic temperature, T	1369.02	(°C)	[11]
Eutectic composition	24.5	(at.% Al)	[11]
Contact angle for γ′, $\theta_{\gamma'}$	26.7	(°)	[13]
Contact angle for β, θ_β	1.7	(°)	[13]

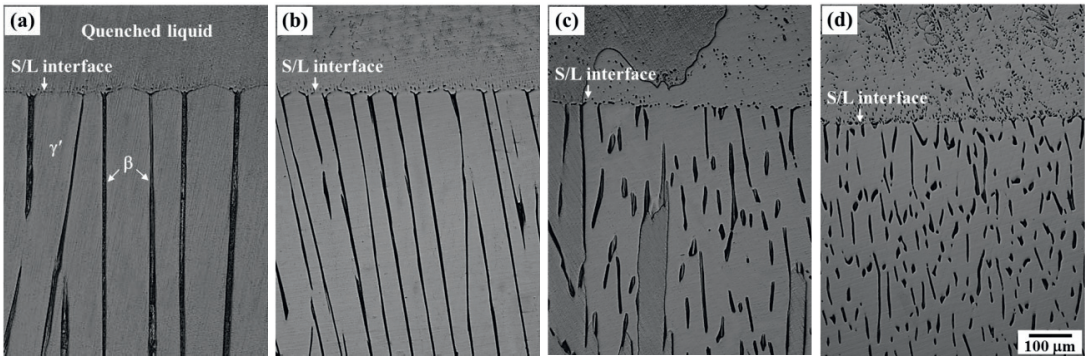

Fig. 2. Longitudinal optical micrographs showing the solid/liquid interface with different growth velocities (magnification: 200×): (a) 1, (b) 5, (c) 10 and (d) 20 μm/s.

3. Results

The microstructural evolution of eutectic phases was examined with different growth rates in the hypereutectic Ni-25.2 at.% Al alloy. Fig. 2 shows the longitudinal microstructures at the solid/liquid interface as a function of growth velocity. The stable eutectic phases composed of the γ′ phase (gray) and β phase (black) were shown to grow isothermally which denotes cooperative growth and the interface microstructure varied from lamellar to rod eutectics with increasing growth velocity.

Fig. 3 shows the transverse microstructures corresponding to the longitudinal micrographs in Fig. 2. The lamellar structure was dominantly observed on the samples grown at low velocities of 1 and 5 μm/s, and the rod eutectic phase was present in a small volume fraction at a growth velocity of 5 μm/s, as shown in Fig. 3(b). This mixed microstructure of lamellae and rods indicates the transition from a lamellar to rod morphology. The volume fraction of the rod phase increased with an increase in growth velocity. The lamellar structure was almost completely transformed into the rod structure when the sample was solidified at the velocity of 20 μm/s, as shown in Fig. 3(d). The spacing of eutectic phases tends to become narrower with increasing growth velocity.

The average spacing of eutectic phases measured for each velocity are logarithmically plotted against growth velocity in Fig. 4. The inter-phase spacing during eutectic growth is determined by a compromise between solute concentration gradients for lateral diffusion and Gibbs-Thomson effect. The relationship between inter-phase spacing λ and growth velocity V was established by Jackson and Hunt [6] who showed that its spacing can be micro-tuned by the minimum undercooling or the maximum growth rate in steady-state conditions: $V\lambda^2 =$ constant. The slope of each line fitted in Fig. 4 is -0.47 for the lamellar structure and -0.49 for the rod structure, respectively and these values agree quite well with the exponent for growth velocity derived above V-λ relationship, i.e. -0.5.

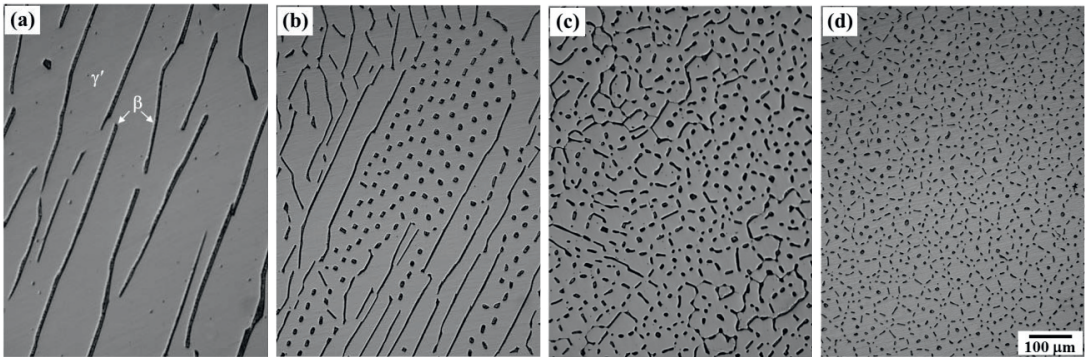

Fig. 3. Transverse microstructures for different growth velocities (magnification: 200×): (a) 1, (b) 5, (c) 10 and (d) 20 μm/s.

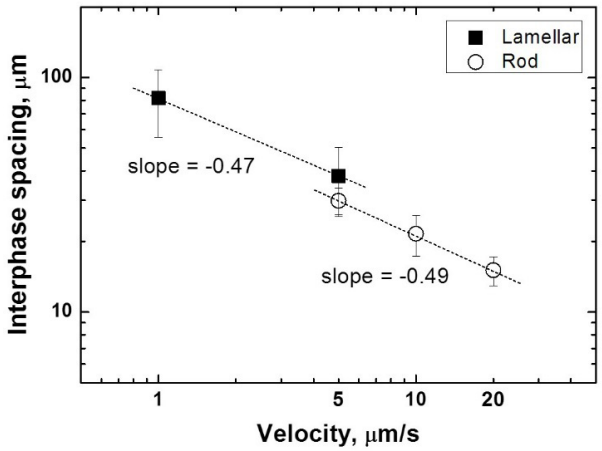

Fig. 4. Variation in average eutectic spacing with growth velocity.

The growth velocity influences on the interface temperature of eutectic phases [6]. However, this behavior is not connected directly with the evolution of the interface morphology. The eutectic morphology depends on the composition in the liquid ahead of the advancing interface or the volume fraction of the minor phase [14]. For the studied Ni-25.2 at.% Al alloy, the rod eutectic structure was stable when the volume fraction of β phase is less than approximately 0.10, whereas the lamellar eutectic tended to form fully when the β volume fraction is approximately 0.19, as presented in Fig. 5. The value of the β volume fraction evaluated from the phase diagram in Fig. 1 is 0.22 for Al = 25.2 at.%. When the volume fraction of one phase is typically less than 0.28, the rod eutectic structure is preferentially selected because of its lower interfacial energy than the other. The discrepancy between the measured and the expected volume fractions can be deduced from the following considerations. First, the β phase in the Ni-Al systems possesses high entropy of fusion, $\Delta S/R \approx 2$ [15] where ΔS is the entropy of fusion and R is the gas constant. As the minor β phase is nearly faceted, the lamellar structure is able to form at such a low volume fraction, $f_\beta \approx 0.19$. Another contribution to the low volume fraction of β phase is estimated to arise from the quick transformation of β to γ′ phase during water-quenching. The previous studies [13,15] showed that γ and β phases in the Ni-Al systems can be quickly transformed into γ′ phase even at high cooling rates.

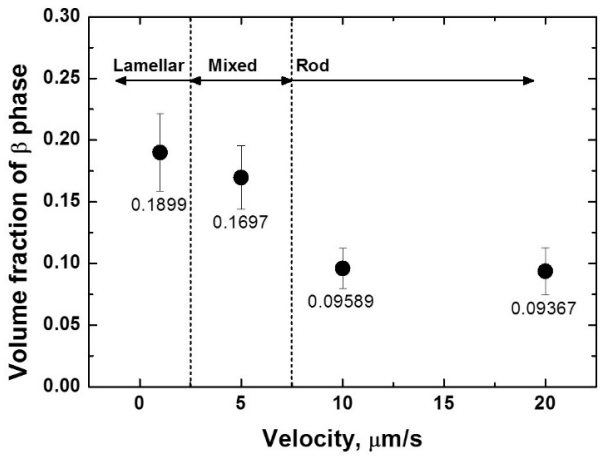

Fig. 5. Variation in the β volume fraction with growth velocity.

Meanwhile, for the alloys in the slightly hypereutectic condition, the liquid composition ahead of the eutectic front can be shifted from hypereutectic to eutectic under certain solidification conditions. To identify the morphological change with composition, Al concentration in β phase was measured as a function of velocity. The composition analysis presented in Fig. 6 shows that the composition change with increasing velocity can be accompanied by the variation in the eutectic morphology. This compositional change is thought to stem from the melt convection in the 5-mm-diameter alumina tube.

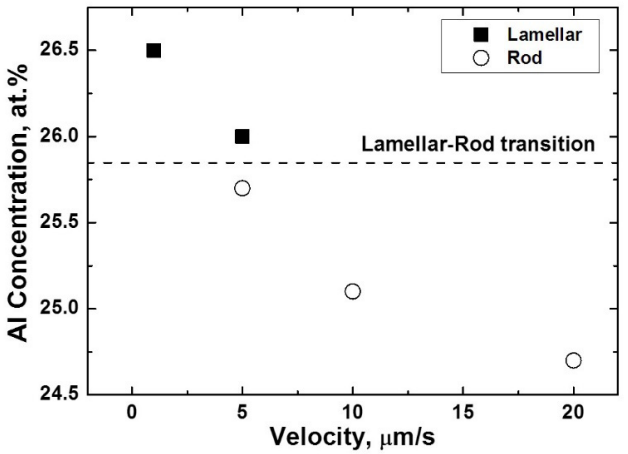

Fig. 6. Variation in composition of eutectic phases with growth velocity.

4. Discussion

For the hypereutectic Ni-25.2 at.% Al alloy, Ni is the solute rejected from the interface and it is even richer than Al. As Al has a low density that is approximately one-third the density of Ni, it can be effectively transferred to the liquid away from the interface by buoyancy-driven convection. The amount of Al segregation in the vertical direction decreases with an increase in growth velocity since there is not enough time to deliver the Al element upwards at high velocities. Therefore, the composition of the melt gets close to the initial alloy composition with increasing growth velocity.

The advancing interface selects a microstructure growing at the highest temperature. In order to figure out the microstructure selection in the Ni-25.2 at.% Al alloy, the interface temperature was calculated by the Jackson-Hunt model [6]. As the alloy composition was changed as a function of the growth velocity as in Fig. 6, the growth temperature for the lamellar structure was compared with that for the rod structure under the given velocity. The growth temperatures for the eutectic structures decreased with increasing growth velocity, as shown in Fig. 7. At velocities of 1 and 5 μm/s, the gap between the interface temperatures for both structures was very small but the interface temperature for the lamellar structure was slightly higher than that for the rod structure. This corresponds to the high volume fraction of β lamellae in the microstructures shown in Figs. 3(a) and (b). On the other hand, the rod structure is shown to grow at higher temperatures than the lamellar structure at velocities of 10 and 20 μm/s. The difference between the interface temperatures for the lamellar and rod structures became remarkable with increasing growth velocity. The basic reason for microstructural changes in the Ni-25.2 at.% Al alloy is that the local composition at the eutectic interface varies with growth velocity, albeit the eutectic morphology changed with the increasing velocity. The interface morphology can be thus determined by the local composition during solidification. The calculated results of eutectic interface temperature in Fig. 7 verify that in spite of the little difference in composition between γ′ phase and β phase, the γ′-β eutectic morphology during solidification can be transformed by small changes in the melt composition induced by natural convection.

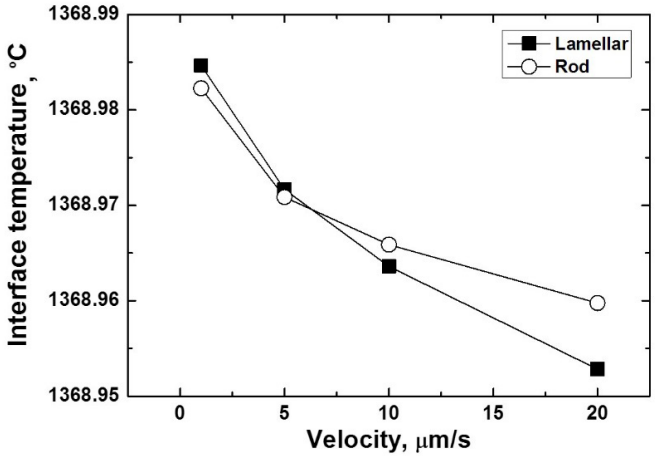

Fig. 7. Interface temperatures of lamellar and rod eutectics with growth velocity.

The spacing selection of eutectic phases is hardly governed by the minimum undercooling condition [7]. The stable eutectic array can be present in a range of spacing value for a given growth velocity. If the eutectic spacing is smaller than λ_m, where λ_m is the spacing corresponding to the minimum undercooling value, it becomes unstable since the minor phase with small volume fraction disappears by the depletion of the interface shape. However, if the eutectic spacing is larger than λ_M, equal to $2\lambda_m$, where λ_M is the spacing corresponding to the maximum undercooling value, it might not grow in a steady-state condition since the spacing control takes place in forming the pocket in the center of the wider phase [6]. The experimentally observed inter-lamellar and -rod spacings are 1.6 times larger than the minimum spacing for each growth velocity, as shown in Fig. 8. Therefore, it appears that the eutectic phases observed at respective velocities have been kept stable since the eutectic spacing was selected at a value between the minimum and the maximum.

5. Conclusion

The effect of growth velocity on the competitive growth between the lamellar and rod eutectic microstructures has been investigated with the hypereutectic Ni-25.2 at.% Al alloy directionally solidified at a constant thermal gradient of 10.0 K/mm. The stable γ′+β eutectic morphologically changed from lamellar to rod structures with increasing velocity in the experimental range of growth velocity between 1 and 20 μm/s. A fully lamellar microstructure was formed at a velocity of 1 μm/s with the β volume fraction of about 0.19 and a rod structure was stable at a very low volume fraction, $f_\beta \approx 0.19$. This low β volume fraction is believed to originate from the interface kinetics of β phase and the phase transformation from β to γ′ phase occurred during quenching. The inter-phase spacing versus growth velocity plot satisfied the Jackson-Hunt relationship: $V\lambda^2$ = constant and further $\Delta T^2/V$= constant.

A decrease in concentration of Al element with increasing growth velocity may explain the microstructural evolution from the lamellae to the rods. The Al concentration in eutectic phases was varied from hypereutectic to eutectic composition. A corresponding result was obtained from the calculation of interface temperature. The eutectic structure with the highest interface temperature was preferentially selected, i.e. the lamellar eutectic gained a lead at a low velocity of 1 μm/s and the rod eutectic for relatively faster velocities more than 10 μm/s. Besides, the spacing selection was made at a critical value 1.6 times larger than the spacing corresponding to the minimum undercooling for each velocity.

Finally, it is unclear why γ′ cell-like structure plus β rods formed in the range of high velocity more than 10 μm/s. These kind of microstructures are often found in the composition range extended approximately from Ni-23 at.% Al

to Ni-27 at.% Al. Experiments related to this behavior are currently in progress to investigate the competitive growth mechanism under imposed solidification conditions.

Acknowledgements

This research was financially supported by the National Research Foundation of Korea (NRF) funded by the Korea government (MSIP) (No. 2011-0030058) and by the Power Generation & Electricity Delivery of the Korea Institute of Energy Technology Evaluation and Planning (KETEP) grants funded by the Korea Ministry of Knowledge Economy (2011T100200224).

References

[1] I.M.S. Sidawi, S.N. Tewari, J. Cryst. Growth 131 (1993) 230-238.
[2] C. Le Marec, R. Guérin, P. Haldenwang, J. Cryst. Growth 169 (1996) 147-160.
[3] A. Rouzaud, D. Camel, J.J. Favier, J. Cryst. Growth 73 (1985) 149-166.
[4] R. Trivedi, H. Miyahara, P. Mazumder, E. Simsek, S.N. Tewari, J. Cryst. Growth 222 (2001) 365-379.
[5] R. Trivedi, P. Mazumder, S.N. Tewari, Metall. Mater. Trans. A 33 (2002) 3763-3775.
[6] K.A. Jackson, J.D. Hunt, Trans. Met. Soc. AIME 236 (1966) 1129-1142.
[7] R. Trivedi, J.T. Mason, J.D. Verhoeven, W. Kurz, Metall. Trans. A 22 (1991) 2523-2533.
[8] H. Walker, S. Liu, J.H. Lee, R. Trivedi, Metall. Mater. Trans. A 38 (2007) 1417-1425.
[9] J. Liu, R. Elliot, Acta Metall. Mater. 43 (1995) 3301-3311.
[10] J.H. Lee, S. Liu, R. Trivedi, Metall. Mater. Trans. A 36 (2005) 3111-3125.
[11] O. Hunziker, W. Kurz, Metall. Mater. Trans. A 30 (1999) 3167-3175.
[12] F. Long, Y.S. Yoo, S.M. Seo, T. Jin, Z.Q. Hu, C.Y. Jo, J. Mater. Sci. Technol. 27 (2011) 101-106.
[13] J.H. Lee, J.D. Verhoeven, J. Cryst. Growth 143 (1994) 86-102.
[14] W. Kurz, D.J. Fisher, Fundamentals of Solidification, third ed., Trans Tech Publications, Vermont, 1989.
[15] O.Hunziker, W. Kurz, Acta Mater. 45 (1997) 4981-4992.